JOC Article

Mechanism of Metal Chloride-Promoted Mukaiyama Aldol Reactions

Chiong Teck Wong and Ming Wah Wong*

Department of Chemistry, National University of Singapore, 3 Science Drive 3, Singapore 117543, Singapore

chmwmw@nus.edu.sg

Received October 25, 2006

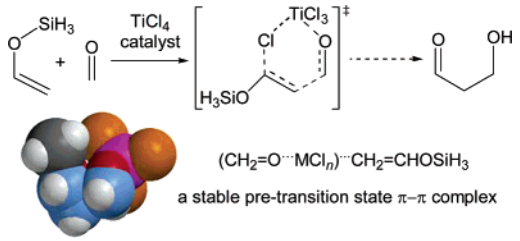

Ab initio calculations (MP2/6-311+G**//B3LYP/6-31G*) were employed to investigate the mechanism of metal chloride-promoted Mukaiyama aldol reaction between trihydrosilyl enol ether and formaldehyde. The metal chlorides considered include $TiCl_4$, BCl_3, $AlCl_3$, and $GaCl_3$. In contrast to the concerted pathway of the uncatalyzed aldol reaction, the Lewis acid-promoted reactions favor a stepwise mechanism. Three possible stepwise pathways were located. The lowest energy pathway corresponds to a simultaneous C−C bond formation and a chlorine atom shift in the first (rate-determining) step. This process is calculated to have a low activation barrier of 12 kJ mol^{-1} for the $TiCl_4$-promoted reaction. The alternative [2+2] cycloaddition and direct carbon−carbon bond formation pathways are energetically competitive. BCl_3, $AlCl_3$, and $GaCl_3$ are predicted to be efficient catalysts for the silicon-directed aldol reaction as they strongly activate the formaldehyde electrophile. Formation of a stable pretransition state intermolecular $\pi-\pi$ complex between enol silane and the activated formaldehyde (CH_2═O···MCl_n) is a key driving force for the facile metal chloride-promoted reactions.

Introduction

The Mukaiyama aldol reaction[1] is a versatile carbon−carbon bond formation process that provides a synthetic pathway to β-hydroxycarbonyl compounds. Besides the original $TiCl_4$ catalyst reported by Mukaiyama[1] for addition of silyl enol ethers to carbonyl compounds (Scheme 1), many other catalysts have been developed that give good yields and high enantioselectivities.[2] By incorporating and modifying the substituents on the reactants, this silicon-directed aldol reaction also proceeds without a catalyst.[3,4] More recently, Mukaiyama aldol reaction has been extended to phosphorus−carbon bond formation (phospho-Mukaiyama)[5] which has many important applications in biochemistry.

SCHEME 1. The First Mukaiyama Aldol Reaction

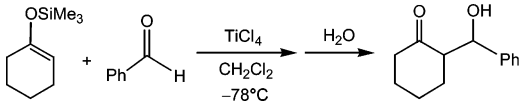

Experimentally, Mukaiyama aldol reaction would normally give rise to one major product: a hydroxy,[1,6] silyl,[7] or (less

(1) (a) Mukaiyama, T.; Banno, K.; Narasaka, K. *J. Am. Chem. Soc.* **1974**, *96*, 7503. (b) Mukaiyama, T.; Izawa, T.; Saigo, K. *Chem. Lett.* **1974**, 323. (c) Mukaiyama, T.; Narasaka, K.; Banno, K. *Chem. Lett.* **1973**, 1011. (d) Mukaiyama, T. *Angew. Chem., Int. Ed.* **1979**, *16*, 817.

(2) (a) *Modern Aldol Reactions*; Mahrwald, R., Ed.; Wiley-VCH: New York, 2004. (b) Palomo, C.; Oiarbide, M.; Garcia, J. M. *Chem. Soc. Rev.* **2004**, *33*, 65. (c) Carreira, E. M. In *Comprehensive Asymmetric Catalyst*; Jacobsen, R. N., Pfaltz, A., Yamamoto, H., Eds.; Springer-Verlag: Berlin, Germany, 1999; Vol. 3. (d) Palomo, C.; Oiarbide, M.; Garcia, J. M. *Chem. Eur. J.* **1998**, *4*, 36. (e) Groger, H.; Vogl, E. M.; Shibasaki, M. *Chem. Eur. J.* **2002**, *8*, 1137. (f) Chan, T.-H. In *Comprehensive Organic Synthesis*; Trost, B. M., Ed.; Pergamon Press: New York, 1991; Vol. 2. (g) Imashiro, R.; Kuroda, T. *J. Org. Chem.* **2003**, *68*, 974. (h) Flowers R. A., II; Xu, X.; Timmons, C.; Li. G. *Eur. J. Org. Chem.* **2004**, 2988. (i) Ooi, T.; Maruoka, K. *Acc. Chem. Res.* **2004**, *37*, 526. (j) Zhuang, W.; Poulsen, T. B.; Jorgensen, K. A. *Org. Biomol. Chem.* **2005**, *3*, 3284.

(3) (a) Myers, A. G.; Widdowson, K. L. *J. Am. Chem. Soc.* **1990**, *112*, 9672. (b) Myers, A. G.; Kephart, S. E.; Chen, H. *J. Am. Chem. Soc.* **1992**, *114*, 7922. (c) Denmark, S. E.; Griedel, B. D.; Coe, D. M.; Schnute, M. E. *J. Am. Chem. Soc.* **1994**, *116*, 7026. (d) Denmark, S. E.; Griedel, B. D. *J. Org. Chem.* **1994**, *59*, 5136. (e) Denmark, S. E.; Griedel, B. D.; Coe, D. M. *J. Org. Chem.* **1993**, *58*, 988. (f) Denmark, S. E.; Winter, S. B. D.; Su, X.; Wong, K. T. *J. Am. Chem. Soc.* **1996**, *118*, 7404. (g) Miura, K.; Sato, H.; Tamaki, K.; Ito, H.; Hosomi, A. *Tetrahedron Lett.* **1998**, *39*, 2585. (h) Denmark, S. E.; Fan, Y. *J. Am. Chem. Soc.* **2002**, *124*, 4233.

(4) Wong, C. T.; Wong, M. W. *J. Org. Chem.* **2005**, *70*, 124.

(5) Cain, M. J.; Cawley, A.; Sum, V.; Brown, D.; Thornton-Pett, M.; Kee, T. P. *Inorg. Chim. Acta* **2003**, *345*, 154.

10.1021/jo062218v CCC: $37.00
Published on Web 01/18/2007

SCHEME 2. Concerted Mechanism of the Uncatalyzed Mukaiyama Aldol Reaction

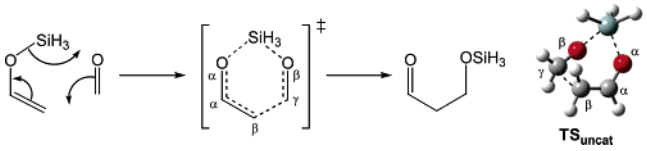

commonly) "ene"[8] product, depending on the type of catalyst used. The reaction conditions (e.g., solvent) are also important in determining the nature of product.[9] For instance, Takasu et al.[10] have reported the preference for the formation of a [2+2] cycloaddition product over the Mukaiyama aldol product in their study of the Lewis acid-catalyzed reactions between silyl enol ethers and α,β-unsaturated ethers.

Various plausible mechanisms have been proposed to account for the catalyzed Mukaiyama aldol reactions.[2d,11−15] However, to date, the actual mechanism has not been determined conclusively. In contrast to the concerted cyclic transition state for the uncatalyzed reactions,[4,16] it is generally believed that the Lewis acid-catalyzed reactions take place by way of an open, less organized transition state. In some cases, an intermediate has been isolated and characterized. For instance, a [2+2] addition intermediate has been observed by Ellis and Bosnich for reactions involving a chiral europium catalyst.[12] Solid-state characterization of a trichlorotitanium aldolate has been reported by Cozzi and Floriani.[13] Several authors have suggested that certain metal catalysts used in Mukaiyama aldol reactions are not necessarily the "actual catalysts". These metal catalysts may generate an $SiMe_3X/SiMe_3^+$ intermediate species, which in turns serves as the actual catalyst in the aldol addition.[14] On the basis of extensive crossover, kinetic, and stereochemical experiments, Denmark and Chen have concluded that the catalytic species in their silicon-directed aldol reaction is that of triarylcarbenium ions.[15]

It is commonly accepted that Lewis acid catalyst activates a carbonyl substrate (electrophile) by coordinating to the carbonyl oxygen, rending it more susceptible to a nucleophilic attack by enol silane. Unexpectedly, in a recent study of silver(I)-catalyzed Mukaiyama aldol reactions, Ohkouchi et al.[17] have shown that the silver(I) carboxylate-BINAP catalyst coordinated to the nucleophile, in which this activated complex then attacks the aldehyde to afford the aldol adduct. With the vast range of catalysts and reaction conditions being investigated in the literature, it is unlikely that all the Mukaiyama aldol reactions proceed via a common reaction pathway. Various experimental studies suggest that the mechanism involved is likely to depend on the Lewis acid properties of the catalyst.

In general, the $TiCl_4$-catalyzed Mukaiyama aldol reaction yielded a hydroxy (not silyl) compound as the main product.[1,13,18] High product yields were obtained when a stoichiometric amount of $TiCl_4$ were used in the presence of a nonpolar solvent.[1] Since the $TiCl_4$ catalyst was not fully recovered in most of the Mukaiyama aldol reactions studied, we prefer to name these reactions as "$TiCl_4$-promoted" reactions. In a recent study, we have examined in detail the mechanism and the governing factors influencing the uncatalyzed Mukaiyama aldol reactions.[4] To extend our study to the catalyzed (or promoted) reactions, we report here a theoretical investigation on the possible mechanisms of metal chloride-promoted reactions between trihydrosilyl enol ether and formaldehyde. The catalysts examined include $TiCl_4$, BCl_3, $AlCl_3$, and $GaCl_3$. To the best of our knowledge, this is the first ab initio study on the promoted Mukaiyama aldol reactions. Understanding the mechanism of these simple metal halide catalysts is essential to comprehend the mechanistic aspects of more complex catalysts, which will aid in the design of more efficient catalysts with high reactivity and enantioselectivity.[19] The enantioselective aspect of the Mukaiyama aldol reaction will not be explored here as it is highly dependent on the position and type of substituents on the reactants.[20]

Computational Methods

Geometry optimizations were performed for all equilibrium structures and transition states with use of the B3LYP[21] hybrid density functional theory (DFT) method with the 6-31G* basis set. The B3LYP/6-31G* optimized geometries were verified to be equilibrium structures or transition states via frequency calculations. An equilibrium structure is characterized by all real frequencies while a transition state has one and only one imaginary frequency. The identities of several key transition states were confirmed by intrinsic reaction coordinate (IRC) calculations. Higher level relative energies were obtained through MP2 calculations together with a larger 6-311+G** basis set, based on the B3LYP/6-31G* optimized geometries. The MP2 theory is particularly important for reliable energy

(6) (a) Phukan, P. *Synth. Commun.* **2004**, *34*, 1065. (b) Chung, W. J.; Ngo, S. C.; Higashiya, S.; Welch, J. T. *Tetrahedron Lett.* **2004**, *45*, 5403. (c) Yang, B.; Chen, X.; Deng, G.; Zhang, Y.; Fan, Q. *Tetrahedron Lett.* **2003**, *44*, 3535. (d) Morohashi, N.; Hattori, T.; Yokomakura, K.; Kabuto, C.; Miyano, S. *Tetrahedron Lett.* **2002**, *43*, 7769. (e) Zimmer, R.; Peritz, A.; Czerwonka, R.; Schefzig, L.; Reissig, H. *Eur. J. Org. Chem.* **2002**, 3419. (f) Li, H.; Tian, H.; Chen, Y.; Wang, D.; Li, C. *Chem. Commun.* **2002**, 2994.

(7) (a) Chancharunee, S.; Perlmutter, P.; Statton, M. *Tetrahedron Lett.* **2003**, *44*, 5683. (b) Ishihara, K.; Kondo, S.; Yamamoto, H. *Synlett* **1999**, *8*, 1283.

(8) Mikami, K.; Matsukawa, S. *J. Am. Chem. Soc.* **1993**, *115*, 7039.

(9) Munoz-Muniz, O.; Quintanar-Audelo, M.; Juaristi, E. *J. Org. Chem.* **2003**, *68*, 1622.

(10) Takasu, K.; Ueno, M.; Inanaga, K.; Ihara. M. *J. Org. Chem.* **2004**, *69*, 517.

(11) (a) Oisaki, K.; Suto, Y.; Kanai, M.; Shibasaki, M. *J. Am. Chem. Soc.* **2003**, *125*, 5644. (b) Wadamoto, M.; Ozasa, N.; Yanagisawa, A.; Yamamoto, H. *J. Org. Chem.* **2003**, *68*, 5593. (c) Ishii, A.; Kojima, J.; Mikami, K. *Org. Lett.* **1999**, *12*, 2013. (d) Lin, S.; Bondar, G. V.; Levy, C. J.; Collins, S. *J. Org. Chem.* **1998**, *63*, 1885. (e) Denmark, S. E.; Lee, W. *J. Org. Chem.* **1994**, *59*, 707.

(12) Ellis, W. W.; Bosnich, B. *J. Chem. Soc., Chem. Commun.* **1998**, 193.

(13) Cozzi, P. G.; Floriani, C. *Organometallics* **1994**, *13*, 2131.

(14) (a) Ishihara, K.; Hiraiwa, Y.; Yamamoto, H. *Chem. Commun.* **2002**, 1564. (b) Hollis, T. K.; Bosnich, B. *J. Am. Chem. Soc.* **1995**, *117*, 4570. (c) Carreira, E. M.; Singer, R. A. *Tetrahedron Lett.* **1994**, *35*, 4323.

(15) Denmark, S. E.; Chen, C. *Tetrahedron Lett.* **1994**, *35*, 4327.

(16) Gung, B. W.; Zhu, Z.; Fouch, R. A. *J. Org. Chem.* **1995**, *60*, 2860.

(17) (a) Ohkouchi, M.; Masui, D.; Yamaguchi, M.; Yamagishi, T. *J. Mol. Catal. A* **2001**, *170*, 1. (b) Ohkouchi, M.; Yamaguchi, M.; Yamagishi, T. *Enantiomer* **2000**, *5*, 71.

(18) (a) Reetz, M. T.; Raguse, B.; Marth, C. F.; Huegel, H. M.; Bach, T.; Fox, D. N. A. *Tetrahedron* **1992**, *48*, 5731. (b) Gennari, C.; Colombo, L.; Bertolini, G.; Schimperna, G. *J. Org. Chem.* **1987**, *52*, 2754.

(19) (a) Hamza, A.; Schubert, G.; Soos, T.; Papai, I. *J. Am. Chem. Soc.* **2006**, *128*, 13151. (b) Zhang, X.; Houk, K. N. *J. Org. Chem.* **2005**, *70*, 9712. (c) Clemente, R.; Houk, K. N. *Angew. Chem., Int. Ed.* **2004**, *43*, 5766. (d) Rankin, K. N.; Gauld, J. W.; Boyd, R. J. *J. Phys. Chem. A* **2002**, *106*, 5155.

(20) Evans, D. A.; Dart, M. J.; Duffy, J. L.; Yang, M. G. *J. Am. Chem. Soc.* **1996**, *118*, 4322.

(21) (a) Lee, C.; Yang, W.; Parr, R. G. *Phys. Rev. B* **1988**, *37*, 785. (b) Becke, A. D. *J. Chem. Phys.* **1993**, *98*, 5648.

SCHEME 3. Various Possible Pathways of the $TiCl_4$-Promoted Aldol Reaction between Trihydrosilyl Enol Ether and Formaldehyde[a]

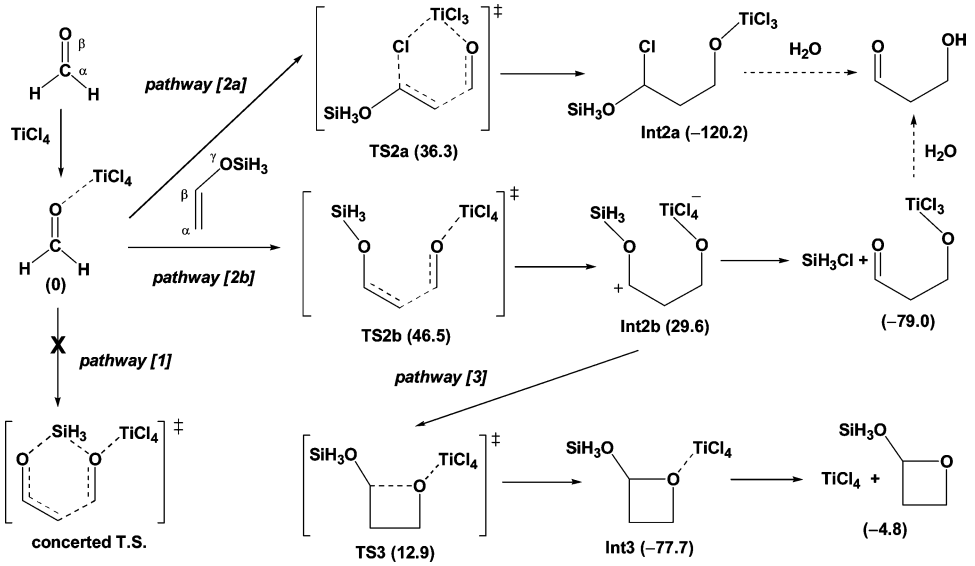

[a] The MP2/6-311+G**//B3LYP/6-31G* relative energies (kJ mol^{-1}) are given in parentheses.

prediction for systems containing $\pi-\pi$ interaction.[22] A scaling factor of 0.9804[23] was used to correct for the directly computed zero-point energies (ZPEs). Unless otherwise noted, the relative energies reported in the text correspond to the MP2/6-311+G** level, including the zero-point energy correction. All calculations were performed with the Gaussian 98[24] suite of programs. Atomic charges were obtained by using the Natural Bond Orbital (NBO) analysis,[25] based on the MP2/6-311+G** wavefunction. Charge density analysis of the intermolecular complexes was performed by using the quantum theory of atoms in molecules (AIM).[26]

Results and Discussion

Uncatalyzed Reaction. Previous studies have shown conclusively that the uncatalyzed silicon-directed aldol reactions proceed via a concerted 6-membered boat-shape transition state (**TS_{uncat}**, Scheme 2).[3c,4,16] This transition state consists of a simultaneous carbon−carbon bond formation and a SiH_3 shift (Scheme 2). Silyl enol ether serves as a nucleophile, while formaldehyde acts as an electrophile. The favorable frontier orbital interaction provides a strong driving force of this concerted process.[4] For the aldol addition between trihydrosilyl enol ether and formaldehyde, the B3LYP/6-31G* level readily reproduces the concerted transition state. The key forming and breaking bond distances of the transition state, 2.100, 1.809, and 1.998 Å for $C_\beta\cdots C_\gamma$, $Si\cdots O_\alpha$, and $Si\cdots O_\beta$, respectively, agree well with the MP2(full)/6-31G* values reported.[4,16] The calculated MP2/6-311+G** barrier (79 kJ mol^{-1}) is in excellent agreement with the higher level G3(MP2) value (77 kJ mol^{-1}).[4] This lends strong confidence to the MP2/6-311+G**//B3LYP/6-31G*+ZPE theory employed here for the metal chloride-promoted aldol reactions.

$TiCl_4$-Promoted Aldol Reaction. First, we examine in detail various plausible reaction mechanisms for the $TiCl_4$-promoted reaction between formaldehyde and trihydrosilyl enol ether (Scheme 3). As expected, $TiCl_4$ forms a stable complex with formaldehyde (Figure 1). On the other hand, the formation of a complex with silyl enol ether is found to be significantly less favorable (binding energy to enol silane = −10 kJ mol^{-1}). The computed binding energy of the $TiCl_4\cdots$formaldehyde complex is −24 kJ mol^{-1}. In this complex, $TiCl_4$ coordinates to formaldehyde oxygen, with a $Ti\cdots O$ distance of 2.345 Å. The C=O bond length of formaldehyde increases from 1.207 to 1.218 Å upon coordination with the $TiCl_4$ catalyst. There is a significant degree of charge transfer, 0.10 e (based on NBO analysis), from formaldehyde to $TiCl_4$ in the complex. In addition, the charge on the carbonyl carbon increases from 0.29 to 0.34 (i.e., carbon becomes more electrophilic) upon complexation. More importantly, the LUMO energy of formaldehyde decreases considerably from 1.88 to 0.17 eV upon complexation. The calculated results here confirm that the electrophilicity of formaldehyde is enhanced by the coordination of $TiCl_4$ catalyst. Thus, the activated aldehyde is more susceptible to aldol addition with enol silane. These factors which promote aldol reactivity in terms of the charge distribution and frontier orbital energies parallel those reported in our recent study for the uncatalyzed

(22) (a) Kurita, N.; Tanaka, S.; Itoh, S. *J. Phys. Chem. A* **2000**, *104*, 8114. (b) Tsuzuki, S.; Luthi, H. P. *J. Chem. Phys.* **2001**, *114*, 3949. (c) Ujaque, G.; Lee, P. S.; Houk, K. N.; Hentemann, M. F.; Danishefsky, S. *Chem. J. Eur.* **2002**, *8*, 3423. (d) Kurita, N.; Sekin. H. *Int. J. Quantum Chem.* **2003**, *91*, 355. (e) Ye, X.; Li, Z.-H.; Wang, W.; Fan, K.; Xu, W.; Hua, Z. *Chem. Phys. Lett.* **2004**, *397*, 56.

(23) Wong, M. W. *Chem. Phys. Lett.* **1996**, *256*, 391.

(24) Frisch, M. J.; Trucks, G. W.; Schlegel, H. B.; Scuseria, G. E.; Robb, M. A.; Cheeseman, J. R.; Zakrzewski, V. G.; Montgomery, J. A., Jr.; Stratmann, R. E.; Burant, J. C.; Dapprich, S.; Millam, J. M.; Daniels, A. D.; Kudin, K. N.; Strain, M. C.; Farkas, O.; Tomasi, J.; Barone, V.; Cossi, M.; Cammi, R.; Mennucci, B.; Pomelli, C.; Adamo, C.; Clifford, S.; Ochterski, J.; Petersson, G. A.; Ayala, P. Y.; Cui, Q.; Morokuma, K.; Malick, D. K.; Rabuck, A. D.; Raghavachari, K.; Foresman, J. B.; Cioslowski, J.; Ortiz, J. V.; Baboul, A. G.; Stefanov, B. B.; Liu, G.; Liashenko, A.; Piskorz, P.; Komaromi, I.; Gomperts, R.; Martin, R. L.; Fox, D. J.; Keith, T.; Al-Laham, M. A.; Peng, C. Y.; Nanayakkara, A.; Gonzalez, C.; Challacombe, M.; Gill, P. M. W.; Johnson, B.; Chen, W.; Wong, M. W.; Andres, J. L.; Gonzalez, C.; Head-Gordon, M.; Replogle, E. S.; Pople, J. A. *Gaussian 98*; Gaussian, Inc.: Pittsburgh, PA, 1998.

(25) Glendening, E. D.; Reed, A. E.; Carpenter, J. E.; Weinhold F. *NBO* Version 3.1.

(26) Bader, R. F. W. *Atoms in Molecules—A Quantum Theory*; Oxford Science Publications: Oxford, UK, 1990.

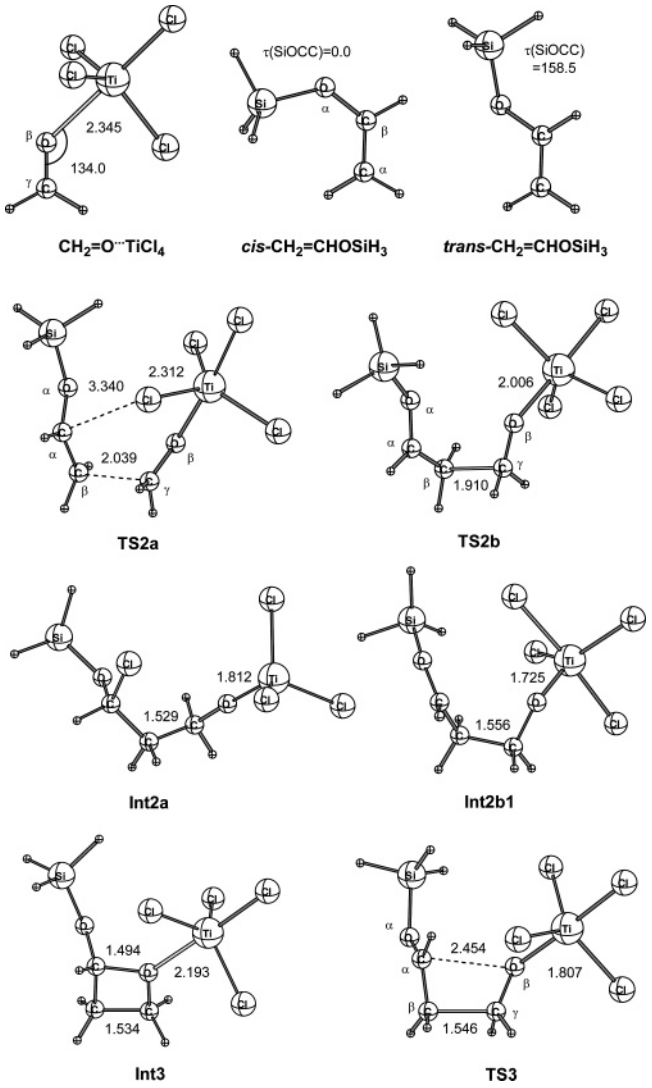

FIGURE 1. Optimized (B3LYP/6-31G*) geometries of various equilibrium and transition structures associated with the $TiCl_4$-promoted aldol reaction between trihydrosilyl enol ether and formaldehyde (bond distances in Å and angles in deg).

silicon-directed aldol reactions.[4] Unless otherwise noted, the total energy of the activated formaldehyde (i.e., $CH_2{=}O{\cdots}TiCl_4$) and enol silane is used as a reference to compute the relative energies in subsequent sections.

Next, we examine the various plausible reaction pathways for the aldol formation between the activated formaldehyde ($CH_2{=}O{\cdots}TiCl_4$) and trihydrosilyl enol ether. We have investigated both the concerted and stepwise processes (Scheme 3). In distinct contrast to the uncatalyzed reaction,[4,16] we were unable to locate a concerted transition structure between the activated formaldehyde complex and enol silane (pathway 1). This result is not unexpected as various experimental studies have indicated a nonconcerted pathway for the catalyzed (or promoted) Mukaiyama reactions.[18,27] For the stepwise process involving the formation of the C−C bond between the carbonyl carbon (C_γ) of the formaldehyde complex and the methylene carbon (C_β) of enol silane, we found two possible reaction pathways: pathway 2a and pathway 2b.

Pathway 2a involves a simultaneous C−C bond formation and a chlorine shift, via transition state **TS2a** (Figure 1), to form an intermediate **Int2a** (Figure 1). Formation of this intermediate is a strongly exothermic reaction, −120 kJ mol^{-1} with respect to $CH_2{=}O{\cdots}TiCl_4 + CH_2{=}CHOSiH_3$. This process is inhibited by a small activation barrier of 36 kJ mol^{-1} (12 kJ mol^{-1} with respect to the separated reactants and catalyst). The $C_\beta{\cdots}C_\gamma$ and $C_\alpha{\cdots}Cl$ forming bond lengths in **TS2a** are 2.039 and 3.340 Å, respectively (Figure 1). It is worth noting that a similar intermediate does not exist in the uncatalyzed reaction.[4] **Int2a** can readily undergo hydrolysis to give a final hydroxy product. The hydrolysis reaction is a strongly exothermic process (−161.3 kJ mol^{-1}). The various subsequent steps leading to the final product are summarized in the Figure S1 (Supporting Information). Essentially, the first step, via **TS2a**, is the rate-determining step for pathway 2a.

The alternative pathway 2b involves a direct $C_\beta{-}C_\gamma$ bond formation, via **TS2b** (Figure 1), to yield an intermediate **Int2b**. Formation of **Int2b** is a slightly endothermic process (30 kJ mol^{-1}) and associates with an activation barrier of 47 kJ mol^{-1}. **Int2b** intermediate can undergo a SiH_3Cl elimination reaction to give $TiCl_3OCH_2CH_2CH{=}O$ (reaction energy = −109 kJ mol^{-1}), which may then undergo hydrolysis to give the final hydroxy product (Figure S1, Supporting Information). Interestingly, **TS2b** adopts a *gauche* conformation ($\tau C_\alpha C_\beta C_\gamma O_\beta$ = −58.5°), which may be attributed to the Coulomb attraction between one of the chlorine atoms and the vinyl (or silyl) hydrogen. As with pathway 2a, the first step, via **TS2b**, is the rate-determining step for pathway 2b. We note that Reetz et al.[18a] and Gennari et al.[18b] have indeed observed the formation of $Si(CH_3)_3Cl$ in their mechanistic studies of the $TiCl_4$-catalyzed silicon-directed aldol reactions using NMR spectroscopy. Pathway 2b requires a slightly higher overall activation barrier than pathway 2a, by 10 kJ mol^{-1} (Scheme 3).

It is important to note that there are two stable conformations of trihydrosilyl enol ether, cis and trans (Figure 1), with almost identical energy.[4] We have considered the reaction pathways for both forms of enol silane and the trans form is found to be slightly more favorable in all three reaction pathways examined. Here, only the reaction energetics associated the trans enol ether are reported in the text.

Experimentally, a [2+2] addition intermediate has been observed for reactions involving a chiral europium catalyst.[12] Thus, it is instructive to examine also the process that give rise to a [2+2] cycloaddition product (pathway 3). As in the case of uncatalyzed aldol reaction,[4] [2+2] cycloaddition leads to a stable oxetane···$TiCl_4$ intermediate (**Int3**, Figure 1). This four-membered ring intermediate is stable with respect to the $CH_2{=}O{\cdots}TiCl_4 + CH_2{=}CHOSiH_3$ by 78 kJ mol^{-1} (102 kJ mol^{-1} with respect to the separated reactants and catalyst). For comparison, the oxetane intermediate is 45 kJ mol^{-1} more stable than the reactants in the uncatalyzed reaction.[4] This result clearly indicates that the oxetane intermediate is stabilized in the presence of a Lewis acid catalyst. The oxetane intermediate is formed by a concerted [2+2] cycloaddition process in the uncatalyzed reaction.[4] In distinct contrast, it is a stepwise process for the $TiCl_4$-promoted reaction, i.e., C−C and C−O bond formations are in two different steps. The first step involves the formation of a $C_\beta{-}C_\gamma$ bond to form **Int2b**, via **TS2b**. Hence, the formation of **Int2b** is a common step for both pathways 2b

(27) (a) Denmark, S. E.; Lee, W. *J. Org. Chem.* **1994**, *59*, 707. (b) Aggarwal, V. K.; Masters, S. J.; Adams, H.; Spey, S. E.; Brown, G. R.; Foubister, A. J. *J. Chem. Soc., Perkin Trans. 1* **1995**, 155. (c) Zhao, C.; Bass, J.; Morken, J. P. *Org. Lett.* **2001**, *3*, 2839. (d) Grimmins, M. T.; King, B. W.; Tabet, E. A.; Chaudhary, K. *J. Org. Chem.* **2001**, *66*, 894.

TABLE 1. Calculated Properties of CH_2═O···MCl_n Complexes[a]

catalyst	IE,[b] kJ mol^{-1}	μ,[c] D	r(C−O), Å	r(O···M), Å	q(C)[d]	q(O)[d]	CT[d,e]	LUMO, eV
none		2.37	1.207		0.29	−0.47		1.88
$TiCl_4$	−23.5	4.95	1.218	2.345	0.34	−0.49	0.10	0.17
BCl_3	−17.9	6.43	1.229	1.678	0.36	−0.44	0.25	0.23
$AlCl_3$	−103.0	6.77	1.227	1.979	0.38	−0.54	0.14	0.11
$GaCl_3$	−77.4	6.88	1.224	2.079	0.50	−0.67	0.12	0.20

[a] MP2/6-311+G**//B3LYP/6-31G* level unless otherwise noted. [b] Interaction energy (IE) computed at the MP2/6-311+G**//B3LYP/6-31G*+ZPE level. [c] Dipole moment (μ). [d] Atomic charge based on NBO analysis. [e] Charge transfer (CT) from formaldehyde to metal chloride.

and 3. In the second step, closure of the $C_\alpha-O_\beta$ bond, via **TS3** (Figure 1), forms **Int3**. The relative energies of **TS2b** and **TS3** are 47 and 13 kJ mol^{-1}, respectively. Thus, the formation of **Int2b** is the rate-determining step of pathway 3.

The calculated relative energies of the three possible reaction pathways, namely pathways 2a, 2b, and 3, are summarized in a schematic energy diagram as shown in Scheme 3. It is clear that pathway 2a is the lowest energy pathway. Hence, we conclude that $TiCl_4$-promoted Mukaiyami aldol is a stepwise process, in sharp contrast to the concerted uncatalyzed reaction. The stepwise mechanism involves a simultaneous C−C bond formation and Cl shift in the rate-determining step, with a calculated barrier of just 12 kJ mol^{-1}. This activation barrier is substantially less than the corresponding uncatalyzed aldol reaction (79 kJ mol^{-1} at the same level of theory). This calculated result is accord with the experimental finding that the $TiCl_4$-catalyzed aldol reaction occurs readily below room temperature condition.[1] As evidenced in Scheme 3, pathways 2b and 3 are energetically competitive. In particular, [2+2] cycloaddition is a realistic pathway for catalyst that strongly stabilizes the oxetane intermediate.

On the basis of experimental studies, several authors have suggested that the catalytic species involved in the Mukaiyama aldol reaction is that of $Si(CH_3)_3X/Si(CH_3)_3^+$.[14] In our calculated $TiCl_4$ reaction pathway (Scheme 3) and the NMR experiments,[17] SiR_3Cl (R = H or CH_3) is formed. We have explored also the possibility of SiH_3Cl acting as a catalyst in the silicon-directed aldol reaction. The energy barrier is predicted to be 142 kJ mol^{-1}, substantially higher than that associated with **TS2a**. The possibility of SiH_3^+ ($Si(CH_3)_3^+$) acting as a catalyst is small as the reaction was carried out in a nonpolar solvent that is expected to suppress the formation of charged species. In addition, a hydroxy product was obtained experimentally.[1] This effectively rules out $Si(CH_3)_3X/Si(CH_3)_3^+$ involvement as a catalyst at a temperature of −78 °C.

MCl_3-Catalyzed Aldol Reactions (M = B, Al, and Ga). Finally, we explore the effect of other metal chloride (Lewis acid) catalysts, namely MCl_3 (M = B, Al, and Ga), on the energetics of the Mukaiyama aldol reaction between trihydrosilyl enol ether and formaldehyde. Preliminary calculations on the $AlCl_3$-promoted aldol reaction indicate that the general mechanism of the MCl_3-promoted reaction is similar to that of $TiCl_4$ catalyst discussed in the previous section. Hence, we have examined only the rate-determining steps of pathways 2a, 2b, and 3 (Scheme 3) for the three MCl_3 catalysts. Only **TS2a** and **TS2b** were considered as **TS2b** is the transition state of the common rate-determining step for pathways 2b and 3. As with $TiCl_4$, coordination of MCl_3 to formaldehyde leads to a significant change of the carbonyl group structurally and electronically (Table 1). The LUMO energy is substantially lower in all three formaldehyde complexes. Accordingly, the electrophilicity of the carbonyl carbon, as reflected in the NBO atomic charge, is enhanced upon complexation with MCl_3.

TABLE 2. Calculated Properties of Pretransition State Complexes[a] and Activation Barriers ($\Delta E^{\neq}$, kJ Mol^{-1}) for MCl_n-Promoted Aldol Reactions between CH_2═$CHOSiH_3$ and CH_2═O[b]

	pre-TS complex[a,c]				
catalyst	BE	μ	CT	$\Delta E^{\neq}$ (TS2a)[d]	$\Delta E^{\neq}$ (TS2b)[d]
$TiCl_4$	−24.5	4.85	0.04	11.8 (36.3)	22.0 (46.5)
BCl_3	−30.5	8.61	0.29	−26.6 (3.9)	−26.4 (4.1)
$AlCl_3$	−34.3	8.99	0.23	−29.8 (4.3)	−28.7 (5.5)
$GaCl_3$	−33.1	7.86	0.11	−18.3 (14.8)	−15.3 (17.8)

[a] $\pi-\pi$ complex between CH_2═$CHOSiH_3$ and CH_2═O···MCl_n. [b] MP2/6-311+G**//B3LYP/6-31G*+ZPE level. [c] Binding energy (kJ mol^{-1}), dipole moment (μ, D), and charge transfer (from enol silane to formaldehyde···MCl_n) of the intermolecular $\pi-\pi$ complex. [d] Value in parentheses correspond to relative energy with respect to the pretransition state complex + silyl enol ether (i.e., intrinsic barrier).

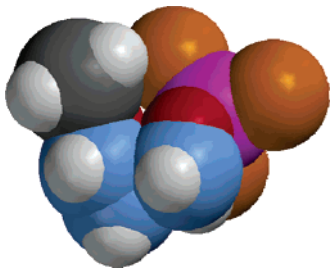

FIGURE 2. The CPK model of the $\pi-\pi$ intermolecular complex between CH_2═O···MCl_3 and *trans*-CH_2═$CHOSiH_3$.

Remarkably, the binding affinities of $AlCl_3$ and $GaCl_3$ to formaldehyde are considerably greater than those of BCl_3 and $TiCl_4$. On the basis of the LUMO energy, one would expect the MCl_3-promoted aldol reaction to have a lower activation barrier. Indeed, the calculated energy barriers (associated with **TS2a** and **TS2b**) are smaller than those of the $TiCl_4$ catalyst (Table 2). Again, pathway 2a, involving a simultaneous C−C bond formation and a Cl shift, is slightly favored over pathway 2b. In sharp contrast to the $TiCl_4$-promoted reaction, the activation barriers are negative in value. How do we account for this unusual result?

Enol silane forms a stable intermolecular complex with the activated formaldehyde (i.e., CH_2═O···MCl_n). This complex is stabilized by the $\pi-\pi$ interaction between the CC π bond of enol silane and the CO π bond of formaldehyde (Figure 2). The $\pi-\pi$ interaction in this complex is particularly strong as enol silane is a strong π donor, while CH_2═O···MCl_n is an effective π acceptor. This is readily reflected in the large degree of charge transfer (0.11−0.29 e) from the enol silane unit to the activated formaldehyde moiety in these $\pi-\pi$ complexes (Table 2). The C···C interaction distance in these π-stacking complexes is in the range 2.41−2.86 Å (Figure 3), similar to those observed in organic molecular crystals of benzene, 3.3−

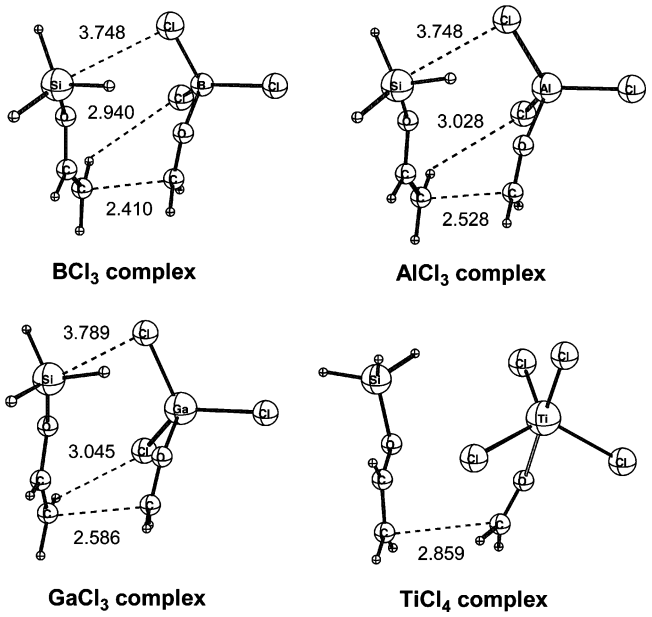

FIGURE 3. Optimized (B3LYP/6-31G*) geometries of the $\pi-\pi$ intermolecular complexes between $CH_2{=}O\cdots MCl_n$ and *trans*-$CH_2{=}CHOSiH_3$ (interaction distances in Å).

3.6 Å.[28] The presence of this $\pi-\pi$ attractive intermolecular force is also supported by charge density analysis, based on the quantum theory of atoms in molecules (AIM).[26] In these complexes, the $\pi-\pi$ interaction is characterized by a bond path and an associated bond critical point (bcp) between C_β of enol silane and C_γ of the formaldehyde−catalyst complex. The calculated bond topological properties, namely the electron density (ρ) and Laplacian of charge density ($\nabla_2\rho$) at the bcp, are similar to those found for the weak intermolecular force such as C−H$\cdots\pi$ interaction.[29] For instance, the ρ and $\nabla_2\rho$ values for the BCl_3 complex are 0.034 and 0.054 au, respectively. The positive $\nabla_2\rho$ indicates the noncovalent nature of interaction. As one might have expected, the $\pi-\pi$ interaction is characterized by a large ellipticity (ϵ) at the bcp, e.g., ϵ = 0.41 for the BCl_3 complex. In the MCl_3 complexes (Figure 3), additional C−H$\cdots$Cl hydrogen bond interaction (2.94−3.05 Å) and Coulomb attraction between the electropositive Si atom and one of the electronegative Cl atoms (3.75− 3.79 Å) of the MCl_3 moiety provide further stabilization in these complexes. Again, the presence of these additional intermolecular forces was confirmed by the AIM topological analysis. The existence of this stable $\pi-\pi$ complex is confirmed by higher level geometry optimizations at MP2/cc-pVTZ and QCISD/6-31G* levels for the BCl_3 complex. The DFT optimized geometry is in good accord with the higher level results.

The computed interaction energies of these pretransition state $\pi-\pi$ complexes are significant, 28−34 kJ mol^{-1}. Indeed, the magnitude is even greater than the intrinsic barrier (Table 2). As a result, the energy barriers of the MCl_3-promoted aldol reactions are negative (Table 2). With respect to the pretransition state complex and enol silane, the intrinsic activation barrier for the aldol reaction (via **TS2a**) is fairly small (<15 kJ mol^{-1}). This is perhaps not surprising as the intermolecular complex bears strong structural resemblance to the transition states. In other words, this pretransition state complex brings the reactants and catalyst in close proximity, and the energy required for structural and electronic re-organization to form the transition state is substantially smaller. Previous studies have shown that pretransition state complex assembly plays a crucial role in understanding the reactivity and enantioselectivity of many Lewis acid-promoted reactions.[30] In the case of $TiCl_4$ catalyst, the interaction energy of the pretransition state complex is relatively smaller and the intrinsic barrier is higher. Consequently, a larger positive barrier is associated with the $TiCl_4$-promoted reaction. It is important to point out that these pretransition state $\pi-\pi$ complexes are characterized by a large dipole moment (Table 2) and are expected to be stabilized in the presence of a dielectric medium. The general mechanism for the MCl_3-promoted aldol reaction is similar to that of the $TiCl_4$ catalyst. Again, the stepwise pathway involves a simultaneous carbon−carbon bond formation and a Cl shift, via **TS2a**, is slightly preferred in all three cases (Table 1). In summary, the formation of a pretransition state complex provides a key driving force of the MCl_n-promoted aldol reactions. The MCl_3 (M = B, Al, and Ga) metal chlorides are predicted to be excellent catalysts for Mukaiyama aldol reactions. The aldol reaction with $AlCl_3$ catalyst was mentioned in a previous study by Mukaiyama.[31] Furthermore, Yamaguchi et al. have successfully employed $GaCl_3$ to promote ethenylation of silylated β-dicarbonyl compound with silylethyne.[32]

Conclusions

We found that the $TiCl_4$-promoted Mukaiyama aldol reaction between trihydrosilyl enol ether and formaldehyde can proceed via three possible stepwise reaction pathways. The lowest energy pathway 2a involves a simultaneous carbon−carbon bond formation and a Cl shift in the rate-determining step, via **TS2a**. The alternative direct carbon−carbon bond formation process (pathway 2b) and the cycloaddition process (pathway 3) are energetic competitive. Our investigation on the catalytic properties of BCl_3, $AlCl_3$, and $GaCl_3$ reveals that these Lewis acids are also effective catalysts for the Mukaiyama aldol reaction with an activation barrier smaller than the TCl_4 catalyst. The MCl_3 catalysts strongly activate the electrophile. The existence of a stable intermolecular $\pi-\pi$ complex between silyl enol ether and the activated formaldehyde ($CH_2{=}O\cdots MCl_n$) provides a crucial driving force of the promoted aldol reactions. We believe that the mechanism of most metal chloride-promoted Mukaiyama aldol reactions which give rise to a hydroxy product will be similar to the mechanism reported here.

Acknowledgment. This research was supported by the National University of Singapore (Grant No. R-143-000-205-112).

Supporting Information Available: Table S1, Cartesian coordinates and absolute energies of all compounds, and Figure S1, schematic energy diagram showing the various possible pathways of $TiCl_4$-promoted aldol reaction between trihydrosilyl enol ether and formaldehyde. This material is available free of charge via the Internet at http://pubs.acs.org.

JO062218V

(28) Dahl, T. *Acta Chem. Scand.* **1994**, *48*, 95.
(29) (a) Ran, J.; Wong, M. W. *J. Phys. Chem. A* **2006**, *110*, 9702. (b) Novoa, J. J.; Mota, F. *Chem. Phys. Lett.* **2000**, *318*, 45.
(30) (a) Corey, E. J. *Angew. Chem., Int. Ed.* **2002**, *41*, 1650. (b).Wong, M. W. *J. Org. Chem.* **2005**, *70*, 5487.
(31) Mukaiyama, T. *Pure Appl. Chem.* **1983**, *11*, 1749.
(32) Arisawa, M.; Akamatsu, K.; Yamaguchi, M. *Org. Lett.* **2001**, *3*, 789.